Investigating Compositional Effects of ALD Ternary Dielectric Ti-Al-O on MISH capacitor structure for Gate Insulation of InAlN/GaN and AlGaN/GaN

Running title: Investigating Compositional Effects of ALD Ternary Dielectric Ti-Al-O on MISH capacitor structure for Gate Insulation of InAlN/GaN and AlGaN/GaN

Running Authors: Colon et al.

Albert Colon

University of Illinois at Chicago, Department of Electrical and Computer Engineering, Suite 1020 SEO, 10th Floor, 851 S Morgan St., Chicago, Illinois 60607

Liliana Stan, Ralu Divan

Argonne National Laboratory, Center for Nanoscale Materials, 9700 S-Cass Ave, Argonne, IL, 60439

Junxia Shi[a)]

University of Illinois at Chicago, Department of Electrical and Computer Engineering, Suite 1020 SEO, 10th Floor, 851 S Morgan St., Chicago, Illinois 60607

[a)] Electronic mail: lucyshi@uic.edu

Gate insulation/surface passivation in AlGaN/GaN and InAlN/GaN heterojunction field-effect transistors (HFETs) is a major concern for passivation of surface traps and reduction of gate leakage current. However, finding the most appropriate gate dielectric materials is challenging and often involves a compromise of the required properties such as dielectric constant, conduction/valence band-offsets or thermal stability. Creating a ternary compound such as Ti-Al-O and tailoring its composition may result in a reasonably good gate material in terms of the said properties. To date, there is limited knowledge of the performance of ternary dielectric compounds on AlGaN/GaN and even less on InAlN/GaN. To approach this problem, we fabricated metal-insulator-

semiconductor heterojunction (MISH) capacitors with ternary dielectrics Ti-Al-O of various compositions, deposited by atomic layer deposition (ALD). The film deposition was achieved by alternating cycles of TiO_2 and Al_2O_3 using different ratios of ALD cycles. TiO_2 was also deposited as a reference sample. The electrical characterization of the MISH capacitors shows an overall better performance of ternary compounds compared to the pure TiO_2. The gate leakage current density decreases with increasing Al content, being ~2-3 orders of magnitude lower for a TiO_2:Al_2O_3 cycle ratio of 2:1. Although the dielectric constant has the highest value of 79 for TiO_2 and decreases with increasing the number of Al_2O_3 cycles, it is maintaining a relatively high value compared to an Al_2O_3 film. Capacitance voltage sweeps were also measured in order to characterize the interface trap density. A decreasing trend in the interface trap density was found while increasing Al content in the film. In conclusion, our study reveals that the desired high-κ properties of TiO_2 can be adequately maintained while improving other insulator performance factors. The ternary compounds may be an excellent choice as a gate material for both AlGaN/GaN and InAlN/GaN based devices.

I. INTRODUCTION

GaN-based metal-insulator-semiconductor heterojunction field-effect transistors (MISHFETs) has received much attention in the research community within the last decades. Due to the wide and direct bandgap nature of the material, there are vast applications for GaN-based devices such as high-power[1], high-frequency[2], photonic devices[3] and more[4]. The optimization of several aspects in the MISHFETs structure has been intensely studied within the recent years. A major topic of interest is the insulator

quality on nitrides. High dielectric constant (κ) insulators are preferred to maintain high transconductance and minimize threshold voltage shift[5] due to the separation of gate-to-channel distance. However, the bandgaps of insulators typically show inverse relation to dielectric constants, i.e. the larger the κ value, the smaller the bandgap. A larger insulator bandgap is preferred to maintain a large conduction/valence band offset to the semiconductor to properly act as a barrier for electrons/holes[6]. Other important desirable properties for an insulator include thermal stability (crystallization temperature), breakdown strength, interface trap density, leakage current, etc. However, commonly used materials such as HfO_2[7, 8] or Al_2O_3[7], involve trade-offs in performance parameters. For example, although TiO_2 may provide a high dielectric constant of 70-90[9, 10], it suffers from poor conduction band offset to GaN[11] and has a low crystallization temperature of 370° C[12]. On the other hand, Al_2O_3 provides adequate band-offsets to GaN[13] and high temperature stability up to 900° C[14] but has a low dielectric constant value of ~9[15]. Creating a ternary compound such as Ti-Al-O and tailoring its composition may result in a reasonably good gate insulating/passivation material in terms of said properties. It has been previously shown[16, 17] that Ti-Al-O compounds provide superior properties such as lower leakage current and higher breakdown strength over TiO_2. Moreover, it has been demonstrated by Youngseo et. al.[16] that by increasing the Al-content in the Ti-Al-O composite, it may increase the bandgap, thus improving the band-offsets to their respective substrates. However, there is limited knowledge on this ternary compound on AlGaN/GaN and InAlN/GaN substrates. ALD is amongst the more popular insulator deposition method due to its highly conformal process and its precise deposition control[18]. Moreover, ALD allows relatively easy control and engineering of multicomponent film

composition. A nanolaminate or composite film can easily be attained by changing the numbers of alternating cycles of each component. In this study, we investigated the compositional effects of Ti-Al-O films prepared by ALD on the electrical properties of MISH capacitors on AlGaN/GaN and InAlN/GaN.

II. EXPERIMENTAL

To characterize insulator quality of Ti-Al-O on GaN, circular MISH capacitors were fabricated. A scanning electron microscope (SEM) image of the completed structure is shown in Figure 1. Device fabrication started with AlGaN/GaN on sapphire and InAlN/GaN on SiC epi-wafers provided by CorEnergy Semiconductor Technology Co. Ltd. and NXP Semiconductors, respectively. An overview of the device fabrication process is described in Figures 2(a-i). Prior to the device mesa isolation, the substrates were ultrasonic cleaned with acetone, methanol and isopropanol. The lithography was accomplished using Raith 150 electron-beam lithography system and using ma-N 2405 (MicroChem Corp.), a negative-resist exposed using a dosage of 220 $\mu C/cm^2$. The device mesa isolation etch was performed by inductively-coupled-plasma reactive ion etching (ICP-RIE, Oxford PlasmaLab 100) using a $Ar/Cl_2/BCl_3$ plasma. The ohmic contact formation was achieved by patterning, metal stack deposition, lift-off, and thermal annealing. For patterning the contacts, a bi-layer process based on polymethylglutarimide/polymethyl methacrylate (PMGI/PMMA) was used. The Si/Ti/Al/Mo/Au (1/15/90/45/55 nm) metal stack was deposited by e-beam evaporation (Varian Electron Beam Evaporation System), and the lift-off was done by ultrasonication in a 1165 remover bath. After a rapid thermal annealing of the ohmic stack at an optimized annealing condition at 825° C in N_2 for 30 s (Rapid Thermal Processor,

Modular Process Technology Corp.), the transfer length measurements (TLM) performed on-chip indicated an average contact resistance of 0.42 Ω·mm for InAlN and 0.48 Ω·mm for AlGaN.

Following the ohmic contact formation, ternary dielectric deposition was achieved by thermal ALD (Arradiance Gemstar). The ALD films were deposited on InAlN/GaN, AlGaN/GaN, and Si witness samples. Prior to loading into the ALD chamber, the samples were treated with a buffered oxide etch (BOE) 10:1 dip followed by deionized water (DIW) rinse. The Ti-Al-O composite films were achieved by alternating TiO_2 and Al_2O_3 cycles. Each TiO_2 and Al_2O_3 cycles were carried out using tetrakis(dimethylamido)titanium (TDMATi)/H_2O and trimethylaluminum (TMA)/H_2O, respectively. All films were deposited at 200° C at a deposition rate of 0.37 Å/cycle for TiO_2 and 1.12 Å/cycle for Al_2O_3. TiO_2 was deposited as a reference control sample. To vary the composition, 1 cycle of Al_2O_3 was followed by a various number of consecutive TiO_2 cycles, i.e. 1-cycle of Al_2O_3 followed by n-cycle(s) of TiO_2. The TiO_2:Al_2O_3 cycle ratios studied were 10:1, 5:1, and 2:1. To achieve the final target thickness of ~24 nm, the super cycles were repeated. The thicknesses of the films were then measured by X-ray reflectivity (XRR) (Bruker D8 Discover) and the elemental composition was determined by X-ray photoelectron spectroscopy (XPS).

Following the insulator deposition, the gate contacts were patterned by e-beam lithography using the bi-layer resist process, e-beam evaporation of Ti/Au (28/110 nm) and metal lift-off. Lastly, to make electrical contact to the covered ohmic contact regions, the insulator films were etched from these regions using RIE.

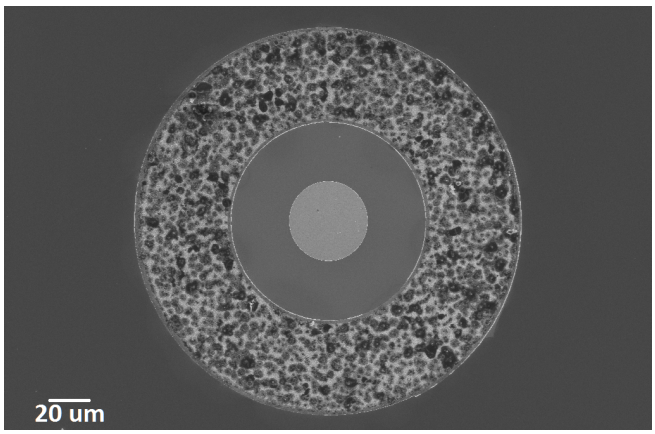


FIG. 1. SEM image of the fabricated circular MISH capacitor.

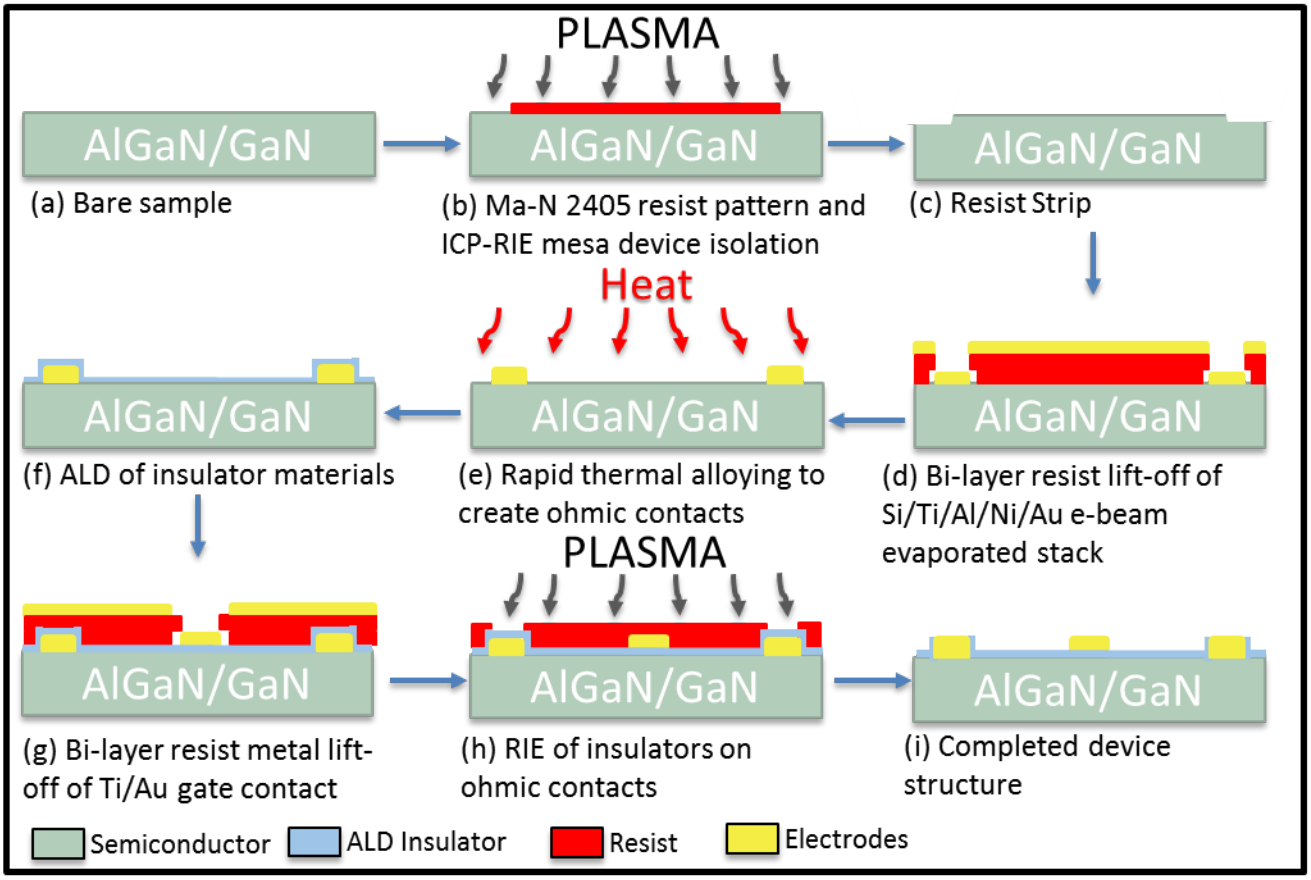


FIG. 2. (Color Online) Schematic cross-section of MISH capacitor fabrication steps. (a) AlGaN(InAlN)/GaN starting epi-wafer. (b) Mesa device isolation is achieved by ICP-RIE using a Cl_2-based plasma. (c) Resist is stripped from the surface. (d) Lift-off of ohmic

metals deposited by E-Beam evaporation. (e) Rapid thermal annealing at 825° C for 30 s in N_2 ambient to create ohmic contact. (f) ALD of ternary insulator materials. (g) Lift-off of gate electrode. (h) RIE of ALD film over ohmic metals. (i) Completed device.

III. RESULTS AND DISCUSSION

Ti-Al-O films of compositions in the TiO_2-rich composition range were grown on the InAlN/GaN and AlGaN/GaN substrates. Their elemental composition was evaluated from the XPS spectra and their thickness from the XRR spectra. The results are summarized in the Table I.

TABLE I. ALD films processing conditions, thickness and composition. 1:0 ratio is the reference TiO_2 film. TiO_2 and Al_2O_3 ratio was varied to produce different Al-content in the films.

Ratio	TiO_2 cycle(s)	Al_2O_3 cycle	Thickness (nm)	Composition
1:0	1	0	24.5	0%
10:1	10	1	26.5	36%
5:1	5	1	27.5	45%
2:1	2	1	28	61%

The X-ray diffraction measurements (not shown) revealed that the amorphous structure of as deposited composite Ti-Al-O films persists in the whole investigated compositional range.

The dielectric properties of the Ti-Al-O films grown on InAlN/GaN and AlGaN/GaN substrates were evaluated through C-V measurements. Leakage current

density was measured for both AlGaN/GaN and InAlN/GaN MISH capacitors and is plotted at gate voltage of -1 V in Figure 3. The TiO_2 reference sample shows a high leakage current which is commonly reported in literature [16, 19, 20]. However, a decreasing trend in leakage current is observed with increasing Al-content in the film. Compared to the pure TiO_2 sample, leakage current was reduced 2-3 orders of magnitude when a 2:1 TiO_2:Al_2O_3 cycle ratio film was used. The InAlN/GaN-based devices show larger leakage values compared to AlGaN/GaN due to the thinner and wider band-gap properties of the InAlN barrier layer.

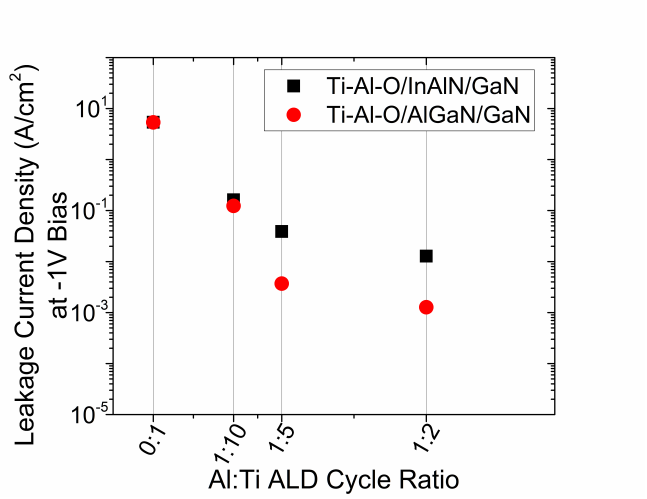


FIG. 3. (Color Online) Leakage current density of the ALD grown Ti-Al-O on InAlN/GaN and AlGaN/GaN as a function of TiO_2:Al_2O_3 ALD cycle ratio measured at a gate bias of -1V. Decreasing leakage current is observed by increasing the Al content in the TiO_2 films.

Figure 4(a) and 4(b) shows the Capacitance-Voltage (C-V) characteristics of the Ti-Al-O dielectrics measured on InAlN/GaN and AlGaN/GaN MISH capacitors, respectively. The voltage was swept from +2 (or +1) to -5 V using a 10 kHz AC signal with 10mV amplitude and .05 V/300 ms step size. A much sharper transition in the

depletion region was observed for the 2:1 TiO_2:Al_2O_3 cycle ratio sample compared to the TiO_2 reference sample. This may be associated with a lower trap density at the insulator/semiconductor interface and our further analysis presented in a later section confirms this assumption. The C-V curve features 2 slopes during the sweep. The 1st slope (at –bias) is associated with the accumulation of electrons at the InAlN(AlGaN)/GaN interface. The 2nd slope (at +bias) shows the spill-over of electrons through the barrier layer onto the insulator/semiconductor interface.

FIG. 4. (Color Online) (a) C-V sweep from +2 to -5 V for the dielectrics measured on InAlN/GaN. (b) C-V sweep from +1 to -5 V for the dielectrics measured on AlGaN/GaN.

Both are measured using an AC signal with 10 kHz frequency, 10 mV amplitude and .05 V step size. The insets show a closer view of the depletion region sweeps.

Dielectric constants were measured through the 0 V bias accumulation capacitance values. For the reference TiO_2 sample, a metal-insulator-metal capacitor was fabricated. From the capacitance measured at low voltage 1 MHz signal, the dielectric constant was directly measured to be 79 which matches well to other reported values[10]. Based on this value, the InAlN barrier layer capacitance was calculated to be ~493 nC/cm^2 from the TiO_2 MISH capacitor. Using this value as a reference for all the samples, the remaining dielectric constant values were calculated using the following equation:

where is the thickness of the insulator, is the permittivity of vacuum, is the area of the MIS gate, is the measured accumulation capacitance of the MISH capacitor, and is the capacitance of the InAlN barrier layer. The results are plotted in Figure 5. Mixing TiO_2 with Al_2O_3 leads to a decrease in the dielectric constant, as expected. The dielectric constant of the sample with 2:1 TiO_2:Al_2O_3 cycle ratio (with Al content of 61 %), is 27 which is relatively high compared to 9, as reported for Al_2O_3[15]. Moreover this value is higher than the dielectric constant of HfO_2, which is widely used as gate dielectric. The composition range of our ALD Ti-Al-O films to maintain a relative high dielectric constant is relatively large.

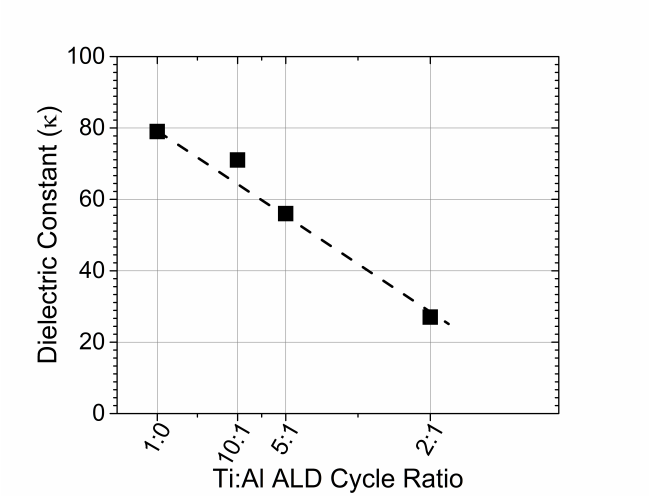


FIG. 5. Calculated dielectric constants of the Ti-Al-O films as a function of TiO_2:Al_2O_3 ALD cycle ratio. Dielectric constant of the TiO_2 is 79 while even at a (2:1) ratio, dielectric constant is maintained at a relatively high value of 27.

The interface between the insulator and semiconductor are filled with interface trapped charges caused by structural defects, impurities and dangling bonds[21]. However, unlike the highly compatible Si-SiO_2 interface, which typically contains interface trap densities[22] (D_{it}) on the order of 10^{11} $eV^{-1}cm^{-2}$, high-κ materials on nitrides suffer from much larger values. It is well known that a high interface trap density causes degradation in device performance such as threshold voltage instability and degradation of 2-DEG mobility[23]. Proper selection of insulator materials based on this criterion is also important. D_{it} values were extracted from the C-V frequency dispersion in the 2nd slope of the C-V sweep using a similar process as reported in literature[24-26]. Based on the onset voltage shift in the 2nd slope (shown in Figure 6), D_{it} values can be calculated for an averaged energy range () using the following equations:

where is the elemental electron charge, is the measured voltage hysteresis between two different frequency sweeps, is the corresponding trap energy difference based on the measurement frequencies and , is Boltzmann's constant, and is measurement temperature. Next, the average activation energy of the traps can be calculated using:

where is the trap activation energy at frequency , is the interface traps capture cross section, is the effective density of states in the barrier conduction band, and is the thermal velocity of electrons.

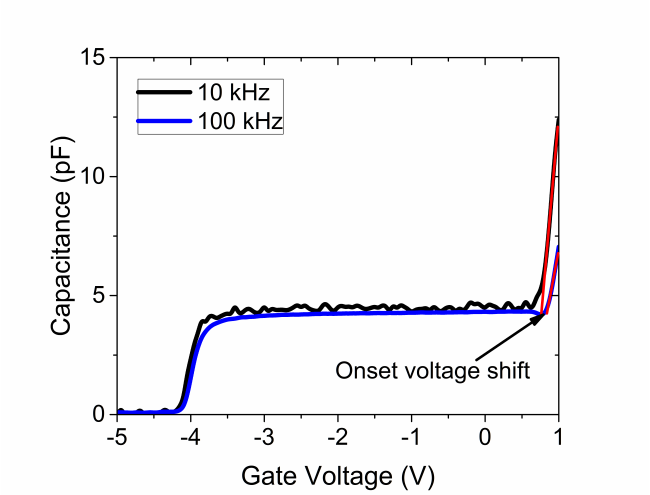


FIG. 6. (Color Online) C-V sweep of TiO_2:Al_2O_3 (2:1) sample measured from AlGaN/GaN MISH capacitor. Based on the onset voltage shift measured from different frequencies in the 2nd slope, trap density values are extracted. Similar plots are measured for InAlN/GaN capacitors but only this plot is shown for clarity.

For the measured frequency range between 1 kHz to 10 kHz, the trap density is measured at the trap activation energy of 0.44 eV below the conduction band edge. The

results are plotted in Figure 7. InAlN/GaN devices show larger trap densities compared to their AlGaN/GaN counterparts. However, the trap density appears to be decreasing with increasing Al-content in the film. From the C-V analysis in Figure 4, it appeared that the TiO_2 sample showed larger stretch-out in the depletion region compared to the Ti-Al-O films, suggesting a worse interface quality of the former, and the D_{it} analysis confirmed these results.

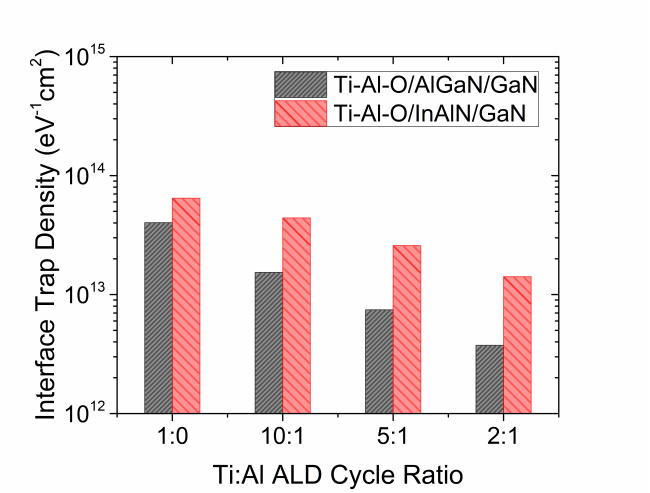


FIG. 7. (Color Online) Interface Trap Density measured from the various MISH capacitor structures. The Ti-Al-O dielectric films on InAlN/GaN appear to have larger interface trap density values compared to their AlGaN/GaN counterparts. Trap densities decrease and show improvement with decreasing TiO_2:Al_2O_3 ratio.

IV. CONCLUSIONS

We investigated the electrical properties of AlGaN/GaN and InAlN/GaN MISH capacitors employing ALD grown ternary Ti-Al-O compounds as the insulator. It was revealed that by increasing the Al-content in the Ti-Al-O film, the leakage current was reduced as much as by ~2-3 orders of magnitude for the Al-Ti-O film with 61 % Al. Regarding the dielectric constant, even for an Al-content of ~61 %, the dielectric constant

was maintained at a relatively high value of 27. The correlations between the interface trap-density of the films and the substrate material and insulator Al-content were also determined through C-V frequency dispersion measurements. The insulators deposited on InAlN/GaN showed larger interface trap densities compared to the AlGaN/GaN counterparts. Also, the ternary compounds showed improvement in this aspect with increasing TiO_2:Al_2O_3 ALD cycle ratio. In conclusion, these ternary compounds may be an excellent choice for GaN-based devices.

ACKNOWLEDGMENTS

The authors would like to thank NXP Semiconductors for the financial support and CorEnergy Semiconductor Technology for the epi-structure supply. The authors would also like to thank Dr. Antonio Divenere and Dr. Seyoung An, staff at the Nanotechnology Core Facility, for their helpful discussions.

Use of the Center for Nanoscale Materials, an Office of Science user facility, was supported by the U. S. Department of Energy, Office of Science, Office of Basic Energy Sciences, under Contract No. DE-AC02-06CH11357.

1. J. Shi, L. F. Eastman, X. Xin and M. Pophristic, Applied Physics Letters **95** (4) (2009).
2. P. Saunier, M. L. Schuette, T.-M. Chou, H.-Q. Tserng, A. Ketterson, E. Beam, M. Pilla and X. Gao, IEEE Trans. Electron Devices **60** (10), 3099-3104 (2013).
3. Y. Nanishi, Nat Photon **8** (12), 884-886 (2014).
4. J. L. Cazaux, S. Forestier, J. F. Villemazet, O. Vendier, C. Schaffauser, C. Drevon and J. L. Muraro, presented at the 2006 Asia-Pacific Microwave Conference, 2006 (unpublished).
5. T.-Y. Wu, C.-C. Hu, P.-W. Sze, T.-J. Huang, F. Adriyanto, C.-L. Wu and Y.-H. Wang, Solid-State Electronics **82**, 1-5 (2013).
6. J. Robertson and B. Falabretti, Journal of Applied Physics **100** (1), 014111 (2006).
7. X. Qin, L. Cheng, S. McDonnell, A. Azcatl, H. Zhu, J. Kim and R. M. Wallace, Journal of Materials Science-Materials in Electronics **26** (7), 4638-4643 (2015).
8. C. Liu, E. F. Chor and L. S. Tan, Applied Physics Letters **88** (17), 173504 (2006).
9. F. Takashi and M. Hiroyuki, Jpn. J. Appl. Phys. **25** (9R), 1288 (1986).
10. F. Hisashi, N. Seigo, M. Miho, I. Yoshihiro, Y. Masaki and N. Shigeru, Jpn. J. Appl. Phys. **38** (10R), 6034 (1999).
11. P. J. Hansen, V. Vaithyanathan, Y. Wu, T. Mates, S. Heikman, U. K. Mishra, R. A. York, D. G. Schlom and J. S. Speck, J. Vac. Sci. Technol. B **23** (2), 499-506 (2005).

12. Q. Xie, J. Musschoot, D. Deduytsche, R. L. Van Meirhaeghe, C. Detavernier, S. Van den Berghe, Y.-L. Jiang, G.-P. Ru, B.-Z. Li and X.-P. Qu, Journal of The Electrochemical Society **155** (9), H688-H692 (2008).
13. R. Suri, North Carolina State University, 2010.
14. S. Jakschik, U. Schroeder, T. Hecht, M. Gutsche, H. Seidl and J. W. Bartha, Thin Solid Films **425** (1–2), 216-220 (2003).
15. S. Ganguly, J. Verma, G. Li, T. Zimmermann, H. Xing and D. Jena, Applied Physics Letters **99** (19), 193504 (2011).
16. A. Youngseo, M. Chandreswar, L. Changmin, C. Sungho, B. Young-Chul, K. Yu-Seon, L. Taeyoon, K. Jiyoung, C. Mann-Ho and K. Hyoungsub, Journal of Physics D: Applied Physics **48** (41), 415302 (2015).
17. J. W. Lim, S. J. Yun and H. T. Kim, Journal of the Electrochemical Society **154** (11), G239-G243 (2007).
18. H. Tiznado, D. Dominguez, W. de la Cruz, R. Machorro, M. Curiel and G. Soto, Revista Mexicana De Fisica **58** (6), 459-465 (2012).
19. W. Lehnert, G. Ruhl and A. Gschwandtner, Journal of Vacuum Science & Technology A **30** (1) (2012).
20. L. C. Haspert, P. Banerjee, L. Henn-Lecordier and G. W. Rubloff, Journal of Vacuum Science & Technology B: Microelectronics and Nanometer Structures **29** (4), 041807 (2011).
21. D. K. Schroder, *Semiconductor Material and Device Characterization*. (Wiley, 2006).
22. E. H. Nicollian and A. Goetzberger, Bell System Technical Journal **46** (6), 1055-1133 (1967).
23. J.-J. Zhu, X.-H. Ma, Y. Xie, B. Hou, W.-W. Chen, J.-C. Zhang and Y. Hao, IEEE Trans. Electron Devices **62** (2), 512-518 (2015).
24. M. Ťapajna, M. Jurkovič, L. Válik, Š. Haščík, D. Gregušová, F. Brunner, E.-M. Cho, T. Hashizume and J. Kuzmík, Journal of Applied Physics **116** (10), 104501 (2014).
25. X. Qin, A. Lucero, A. Azcatl, J. Kim and R. M. Wallace, Applied Physics Letters **105** (1), 011602 (2014).
26. B. Qilong, H. Sen, W. Xinhua, W. Ke, Z. Yingkui, L. Yankui, Y. Chengyue, J. Haojie, L. Junfeng, H. Anqi, Y. Xuelin, S. Bo, L. Xinyu and Z. Chao, Semicond. Sci. Technol. **31** (6), 065014 (2016).

TABLE I. ALD films processing conditions, thickness and composition. 1:0 ratio is the reference TiO_2 film. TiO_2 and Al_2O_3 ratio was varied to produce different Al-content in the films.

				Composition
Ratio	TiO_2 cycle(s)	Al_2O_3 cycle	Thickness (nm)	

1:0	1	0	24.5	0%
10:1	10	1	26.5	36%
5:1	5	1	27.5	45%
2:1	2	1	28	61%

FIG. 1. SEM image of the fabricated circular MISH capacitor.

FIG. 2. (Color Online) Schematic cross-section of MISH capacitor fabrication steps. (a) AlGaN(InAlN)/GaN starting epi-wafer. (b) Mesa device isolation is achieved by ICP-RIE using a Cl_2-based plasma. (c) Resist is stripped from the surface. (d) Lift-off of ohmic metals deposited by E-Beam evaporation. (e) Rapid thermal annealing at 825° C for 30 s in N_2 ambient to create ohmic contact. (f) ALD of ternary insulator materials. (g) Lift-off of gate electrode. (h) RIE of ALD film over ohmic metals. (i) Completed device.

FIG. 3. (Color Online) Leakage current density of the ALD grown Ti-Al-O on InAlN/GaN and AlGaN/GaN as a function of TiO_2:Al_2O_3 ALD cycle ratio measured at a gate bias of -1V. Decreasing leakage current is observed by increasing the Al content in the TiO_2 films.

FIG. 4. (Color Online) (a) C-V sweep from +2 to -5 V for the dielectrics measured on InAlN/GaN. (b) C-V sweep from +1 to -5 V for the dielectrics measured on AlGaN/GaN. Both are measured using an AC signal with 10 kHz frequency, 10 mV amplitude and .05 V step size. The insets show a closer view of the depletion region sweeps.

FIG. 5. Calculated dielectric constants of the Ti-Al-O films as a function of TiO_2:Al_2O_3 ALD cycle ratio. Dielectric constant of the TiO_2 is 79 while even at a (2:1) ratio, dielectric constant is maintained at a relatively high value of 27.

FIG. 6. (Color Online) C-V sweep of TiO_2:Al_2O_3 (2:1) sample measured from AlGaN/GaN MISH capacitor. Based on the onset voltage shift measured from different frequencies in the 2nd slope, trap density values are extracted. Similar plots are measured for InAlN/GaN capacitors but only this plot is shown for clarity.

FIG. 7. (Color Online) Interface Trap Density measured from the various MISH capacitor structures. The Ti-Al-O dielectric films on InAlN/GaN appear to have larger interface trap density values compared to their AlGaN/GaN counterparts. Trap densities decrease and show improvement with decreasing TiO_2:Al_2O_3 ratio.